SLAC–PUB–10777
October 2004

Novel QCD Aspects of Hard Diffraction, Antishadowing, and Single-Spin Asymmetries *

Stanley J. Brodsky
Stanford Linear Accelerator Center
Stanford University, Stanford, California 94309
E-mail: sjbth@slac.stanford.edu

Abstract

It is usually assumed – following the parton model – that the leading-twist structure functions measured in deep inelastic lepton-proton scattering are simply the probability distributions for finding quarks and gluons in the target nucleon. In fact, gluon exchange between the outgoing quarks and the target spectators effects the leading-twist structure functions in a profound way, leading to diffractive leptoproduction processes, shadowing and antishadowing of nuclear structure functions, and target spin asymmetries, physics not incorporated in the light-front wavefunctions of the target computed in isolation. In particular, final-state interactions from gluon exchange lead to single-spin asymmetries in semi-inclusive deep inelastic lepton-proton scattering which are not power-law suppressed in the Bjorken limit. The shadowing and antishadowing of nuclear structure functions in the Gribov-Glauber picture is due respectively to the destructive and constructive interference of amplitudes arising from the multiple-scattering of quarks in the nucleus. The effective quark-nucleon scattering amplitude includes Pomeron and Odderon contributions from multi-gluon exchange as well as Reggeon quark-exchange contributions. Part of the anomalous NuTeV result for $\sin^2\theta_W$ could be due to the non-universality of nuclear antishadowing for charged and neutral currents. Detailed measurements of the nuclear dependence of individual quark structure functions are thus needed to establish the distinctive phenomenology of shadowing and antishadowing and to make the NuTeV results definitive. I also discuss diffraction dissociation as a tool for resolving hadron substructure Fock state by Fock state and for producing leading heavy quark systems.

Presented at the
34th International Symposium on Multiparticle Dynamics (ISMD 2004)
Sonoma State University, Rohnert Park, California
July 26 - August 1, 2004.

*Work supported by Department of Energy contract DE–AC02–76SF00515.

1 Light-Front Wavefunctions and Structure Functions

The concept of a wave function of a hadron as a composite of relativistic quarks and gluons is naturally formulated in terms of the light-front Fock expansion at fixed light-front time, $\tau = x{\cdot}\omega$ Brodsky:1997de. The four-vector ω, with $\omega^2 = 0$, determines the orientation of the light-front plane; the freedom to choose ω provides an explicitly covariant formulation of light-front quantization [2]. The light-front wave functions (LFWFs) $\psi_n(x_i, k_{\perp_i}, \lambda_i)$, with $x_i = \frac{k_i{\cdot}\omega}{P{\cdot}\omega}$, $\sum_{i=1}^n x_i = 1$, $\sum_{i=1}^n k_{\perp_i} = 0_\perp$, are the coefficient functions for n partons in the Fock expansion, providing a general frame-independent representation of the hadron state. Matrix elements of local operators such as spacelike proton form factors can be computed simply from the overlap integrals of light front wave functions in analogy to nonrelativistic Schrödinger theory. In principle, one can solve for the LFWFs directly from the fundamental theory using methods such as discretized light-front quantization, the transverse lattice, lattice gauge theory moments, or Bethe–Salpeter techniques. The determination of the hadron LFWFs from phenomenological constraints and from QCD itself is a central goal of hadron and nuclear physics.

Ever since the earliest days of the parton model, it has been assumed that the leading-twist structure functions $F_i(x, Q^2)$ measured in deep inelastic lepton scattering are determined by the *probability* distributions of quarks and gluons as determined by the light-front wave functions of the target. For example, the quark distribution is

$$P_{\mathrm{q}/N}(x_B, Q^2) = \sum_n \int^{k_{iT}^2 < Q^2} \left[\prod_i dx_i\, d^2k_{Ti}\right] |\psi_n(x_i, k_{Ti})|^2 \sum_{j=q} \delta(x_B - x_j). \qquad (1)$$

The identification of structure functions with the square of light-front wave functions is usually made in the LC gauge, $\omega \cdot A = A^+ = 0$, where the path-ordered exponential in the operator product for the forward virtual Compton amplitude apparently reduces to unity. Thus the deep inelastic lepton scattering cross section appears to be fully determined by the probability distribution of partons in the target.

1.1 The Paradox of Diffractive Deep Inelastic Scattering

A remarkable feature of deep inelastic lepton-proton scattering at HERA is that approximately 10% events are diffractive [3, 4, 5]: the target proton remains intact and there is a large rapidity gap between the proton and the other hadrons in the final state. These diffractive deep inelastic scattering (DDIS) events can be understood most simply from the perspective of the color-dipole model [6]: the $q\overline{q}$ Fock state of the high-energy virtual photon diffractively dissociates into a diffractive dijet system. The color-singlet exchange of multiple gluons between the color dipole of the $q\overline{q}$ and the quarks of the target proton leads to the diffractive final state. The same hard pomeron exchange also controls diffractive vector meson electroproduction at

large photon virtuality [7]. One can show by analyticity and crossing symmetry that amplitudes with $C = +$ hard-pomeron exchange have a nearly imaginary phase.

This observation presents a paradox: deep inelastic scattering is usually discussed in terms of the parton model. If one chooses the conventional parton model frame where the photon light-front momentum is negative $q+ = q^0 + q^z < 0$, then the virtual photon cannot produce a virtual $q\overline{q}$ pair. Instead, the virtual photon always interacts with a quark constituent with light-cone momentum fraction $x = \frac{k^+}{p^+} = x_{bj}$. If one chooses light-cone gauge $A^+ = 0$, then the gauge link associated with the struck quark (the Wilson line) becomes unity. Thus the struck "current" quark experiences no final-state interactions. The light-front wavefunctions $\psi_n(x_i, k_{\perp i}$ of the proton which determine the quark probability distributions $q(x, Q)$ are real since the proton is stable. Thus it appears impossible to generate the required imaginary phase, let alone the large rapidity gaps associated with of DDIS.

This paradox was resolved by Paul Hoyer, Nils Marchal, Stephane Peigne, Francesco Sannino and myself [8]. It is helpful to consider the case where the virtual photon interacts with a strange quark – the $s\overline{s}$ pair is assumed to be produced in the target by gluon splitting. In the case of Feynman gauge, the struck s quark continues to interact in the final state via gluon exchange as described by the Wilson line. The final-state interactions occur at a light-cone time $\Delta\tau \simeq 1/\nu$ after the virtual photon interacts with the struck quark. When one integrates over the nearly-on-shell intermediate state, the amplitude acquires an imaginary part. Thus the rescattering of the quark produces a separated color-singlet $s\overline{s}$ and an imaginary phase.

In contrast, in the case of the light-cone gauge $A^+ = \omega \cdot A = 0$, one must consider the final state interactions of the (unstruck) $\overline{s}$ quark. Light-cone gauge is singular—in particular, the gluon propagator

$$d^{\mu\nu}_{LC}(k) = \frac{i}{k^2 + i\varepsilon}\left[-g^{\mu\nu} + \frac{\omega^\mu k^\nu + k^\mu \omega^\nu}{\omega \cdot k}\right] \tag{2}$$

has a pole at $k^+ = 0$ which requires an analytic prescription. In final-state scattering involving nearly on-shell intermediate states, the exchanged momentum k^+ is of $O\left(1/\nu\right)$ in the target rest frame, which enhances the second term in the propagator. This enhancement allows rescattering to contribute at leading twist even in LC gauge. Thus the rescattering contribution survives in the Bjorken limit because of the singular behavior of the propagator of the exchanged gluon at small k^+ in $A^+ = 0$ gauge. The net result is gauge invariant and identical to the color dipole model calculation.

The calculation of the rescattering effects on DIS in Feynman and light-cone gauge through three loops is given in detail for a simple Abelian model in Ref. [8]. Figure 1 illustrates two LCPTH diagrams which contribute to the forward $\gamma^* T \to \gamma^* T$ amplitude, where the target T is taken to be a single quark. In the aligned jet kinematics the virtual photon fluctuates into a $\mathrm{q\overline{q}}$ pair with limited transverse momentum, and the (struck) quark takes nearly all the longitudinal momentum of the photon. The initial q and $\overline{\mathrm{q}}$ momenta are denoted p_1 and $p_2 - k_1$, respectively. The result is most

easily expressed in eikonal form in terms of transverse distances r_T, R_T conjugate to p_{2T}, k_T. The DIS cross section can be expressed as

$$Q^4 \frac{d\sigma}{dQ^2\, dx_B} = \frac{\alpha_{\rm em}}{16\pi^2} \frac{1-y}{y^2} \frac{1}{2M\nu} \int \frac{dp_2^-}{p_2^-}\, d^2\vec{r}_T\, d^2\vec{R}_T\, |\tilde{M}|^2 \tag{3}$$

where

$$|\tilde{M}(p_2^-, \vec{r}_T, \vec{R}_T)| = \left| \frac{\sin\left[g^2\, W(\vec{r}_T, \vec{R}_T)/2\right]}{g^2\, W(\vec{r}_T, \vec{R}_T)/2} \tilde{A}(p_2^-, \vec{r}_T, \vec{R}_T) \right| \tag{4}$$

is the resummed result. The Born amplitude is

$$\tilde{A}(p_2^-, \vec{r}_T, \vec{R}_T) = 2eg^2 MQ p_2^-\, V(m_{||} r_T) W(\vec{r}_T, \vec{R}_T) \tag{5}$$

where $m_{||}^2 = p_2^- M x_B + m^2$ and

$$V(m\, r_T) \equiv \int \frac{d^2\vec{p}_T}{(2\pi)^2} \frac{e^{i\vec{r}_T \cdot \vec{p}_T}}{p_T^2 + m^2} = \frac{1}{2\pi} K_0(m\, r_T). \tag{6}$$

The rescattering effect of the dipole of the $\mathrm{q\overline{q}}$ is controlled by

$$W(\vec{r}_T, \vec{R}_T) \equiv \int \frac{d^2\vec{k}_T}{(2\pi)^2} \frac{1 - e^{i\vec{r}_T \cdot \vec{k}_T}}{k_T^2} e^{i\vec{R}_T \cdot \vec{k}_T} = \frac{1}{2\pi} \log\left(\frac{|\vec{R}_T + \vec{r}_T|}{R_T} \right). \tag{7}$$

The fact that the coefficient of $\tilde{A}$ in Eq. (4) is less than unity for all $\vec{r}_T, \vec{R}_T$ shows that the rescattering corrections reduce the cross section in analogy to nuclear shadowing.

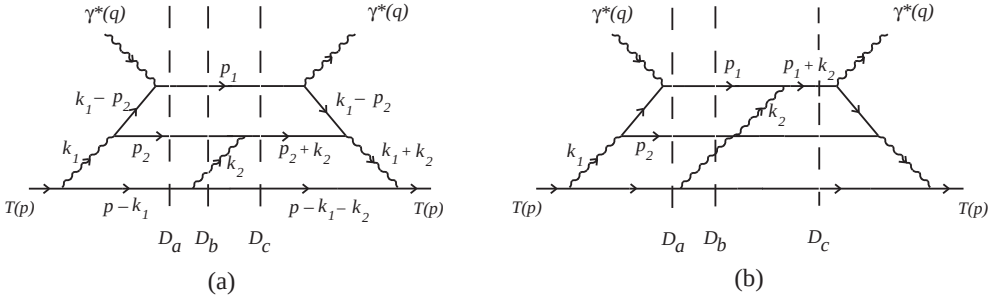

Figure 1: Two types of final state interactions. (a) Scattering of the antiquark (p_2 line), which in the aligned jet kinematics is part of the target dynamics. (b) Scattering of the current quark (p_1 line). For each light-front time-ordered diagram, the potentially on-shell intermediate states—corresponding to the zeroes of the denominators D_a, D_b, D_c—are denoted by dashed lines.

A new understanding of the role of final-state interactions in deep inelastic scattering has thus emerged. The final-state interactions from gluon exchange occurring

immediately after the interaction of the current produce a leading-twist diffractive component to deep inelastic scattering $\ell p \to \ell' p' X$ due to the color-singlet exchange with the target system. This rescattering is described in the Feynman gauge by the path-ordered exponential (Wilson line) in the expression for the parton distribution function of the target. The multiple scattering of the struck parton via instantaneous interactions in the target generates dominantly imaginary diffractive amplitudes, giving rise to an effective "hard pomeron" exchange. The presence of a rapidity gap between the target and diffractive system requires that the target remnant emerges in a color-singlet state; this is made possible in any gauge by the soft rescattering of the final-state $s - \overline{s}$ system.

Rikard Enberg, Paul Hoyer, Gunnar Ingelman and I have recently discussed further aspects of the QCD dynamics of diffractive deep inelastic scattering [9]. We show that the quark structure function of the effective hard pomeron has the same form as the quark contribution of the gluon structure function. The hard pomeron is not an intrinsic part of the proton; rather it must be considered as a dynamical effect of the lepton-proton interaction.

Our QCD-based picture also applies to diffraction in hadron-initiated processes. The rescattering is different in virtual photon- and hadron-induced processes due to the different color environment, which accounts for the observed non-universality of diffractive parton distributions. In the hadronic case the color flow at tree level can involve color-octet as well as color-triplet separation. Multiple scattering of the quarks and gluons can set up a variety of different color singlet domains. This framework also provides a theoretical basis for the phenomenologically successful Soft Color Interaction (SCI) model which includes rescattering effects and thus generates a variety of final states with rapidity gaps.

As I review below, the final-state interactions from gluon exchange between the outgoing quarks and the target spectator system also lead to single-spin asymmetries in semi-inclusive deep inelastic lepton-proton scattering which are not power-law suppressed at large photon virtuality Q^2 at fixed x_{bj} [10]

1.2 The Origin of Nuclear Shadowing and Antishadowing

The physics of nuclear shadowing in deep inelastic scattering can be most easily understood in the laboratory frame using the Glauber-Gribov picture [11, 12, 13]. The virtual photon, W, or Z^0 produces a quark-antiquark color-dipole pair which can interact diffractively or inelastically on the nucleons in the nucleus. The destructive interference of diffractive amplitudes from pomeron exchange on the upstream nucleons then causes shadowing of the virtual photon interactions on the back-face nucleons [14, 15, 16, 17, 18, 19, 20]. The Bjorken-scaling diffractive interactions on the nucleons in a nucleus thus leads to the shadowing (depletion at small x_{bj}) of the nuclear structure functions.

As emphasized by Ioffe [17], the coherence between processes which occur on

different nucleons at separation L_A requires small Bjorken x_B : $1/Mx_B = 2\nu/Q^2 \geq L_A$. The coherence between different quark processes is also the basis of saturation phenomena in DIS and other hard QCD reactions at small x_B [21], and coherent multiple parton scattering has been used in the analysis of $p + A$ collisions in terms of the perturbative QCD factorization approach [22]. An example of the interference of one- and two-step processes in deep inelastic lepton-nucleus scattering illustrated in Fig. 2.

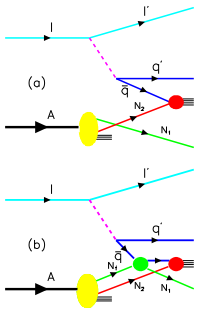

Figure 2: The one-step and two-step processes in DIS on a nucleus. If the scattering on nucleon N_1 is via pomeron exchange, the one-step and two-step amplitudes are opposite in phase, thus diminishing the $\overline{q}$ flux reaching N_2. This causes shadowing of the charged and neutral current nuclear structure functions.

An important aspect of the shadowing phenomenon is that the diffractive contribution $\gamma^* N \to XN'$ to deep inelastic scattering (DDIS) where the nucleon N_1 in Fig. 2 remains intact is a constant fraction of the total DIS rate, confirming that it is a leading-twist contribution. The Bjorken scaling of DDIS has been observed at HERA [4, 23, 24]. As shown in Ref. [8], the leading-twist contribution to DDIS arises in QCD in the usual parton model frame when one includes the nearly instantaneous gluon exchange final-state interactions of the struck quark with the target spectators. The same final state interactions also lead to leading-twist single-spin asymmetries in semi-inclusive DIS [10]. Thus the shadowing of nuclear structure functions is also a leading-twist effect.

It was shown in Ref. [25] that if one allows for Reggeon exchanges which leave a nucleon intact, then one can obtain *constructive* interference among the multi-scattering amplitudes in the nucleus. A Bjorken-scaling contribution to DDIS from Reggeon exchange has in fact also been observed at HERA [4, 24]. The strength and energy dependence of the $C = +$ Reggeon $t-$channel exchange contributions to virtual Compton scattering is constrained by the Kuti-Weisskopf [26] behavior $F_2(x) \sim x^{1-\alpha_R}$ of the non-singlet electromagnetic structure functions at small x. The phase of the Reggeon exchange amplitude is determined by its signature factor. Because of this phase structure [25], one obtains constructive interference and *antishadowing* of the nuclear structure functions in the range $0.1 < x < 0.2$ – a pronounced excess of the

nuclear cross section with respect to nucleon additivity [27].

In the case where the diffractive amplitude on N_1 is imaginary, the two-step process has the phase $i \times i = -1$ relative to the one-step amplitude, producing destructive interference. (The second factor of i arises from integration over the quasi-real intermediate state.) In the case where the diffractive amplitude on N_1 is due to $C = +$ Reggeon exchange with intercept $\alpha_R(0) = 1/2$, for example, the phase of the two-step amplitude is $\frac{1}{\sqrt{2}}(1-i) \times i = \frac{1}{\sqrt{2}}(i+1)$ relative to the one-step amplitude, thus producing constructive interference and antishadowing.

The effective quark-nucleon scattering amplitude includes Pomeron and Odderon contributions from multi-gluon exchange as well as Reggeon quark-exchange contributions [25]. The coherence of these multiscattering nuclear processes leads to shadowing and antishadowing of the electromagnetic nuclear structure functions in agreement with measurements. The Reggeon contributions to the quark scattering amplitudes depend specifically on the quark flavor; for example the isovector Regge trajectories couple differently to u and d quarks. The s and $\overline{s}$ couple to yet different Reggeons. This implies distinct anti-shadowing effects for each quark and antiquark component of the nuclear structure function. Ivan Schmidt, Jian-Jun Yang, and I [28] have shown that this picture leads to substantially different antishadowing for charged and neutral current reactions.

Figs. 3–4 illustrate the individual quark q and anti-quark $\overline{q}$ contributions to the ratio of the iron to nucleon structure functions $R = F_2^A/F_2^{N_0}$ in a model calculation where the Reggeon contributions are constrained by the Kuti-Weisskopf behavior [26] of the nucleon structure functions at small x_{bj}. Because the strange quark distribution is much smaller than u and d quark distributions, the strange quark contribution to the ratio is very close to 1 although s^A/s^{N_0} may significantly deviate from 1.

Our analysis leads to substantially different nuclear antishadowing for charged and neutral current reactions; in fact, the neutrino and antineutrino DIS cross sections are each modified in different ways due to the various allowed Regge exchanges. The non-universality of nuclear effects will modify the extraction of the weak-mixing angle $\sin^2\theta_W$, particularly because of the strong nuclear effects for the F_3 structure function. The shadowing and antishadowing of the strange quark structure function in the nucleus can also be considerably different than that of the light quarks. We thus find that part of the anomalous NuTeV result [29] for $\sin^2\theta_W$ could be due to the non-universality of nuclear antishadowing for charged and neutral currents. Our picture also implies non-universality for the nuclear modifications of spin-dependent structure functions.

Thus the antishadowing of nuclear structure functions depends in detail on quark flavor. Careful measurements of the nuclear dependence of charged, neutral, and electromagnetic DIS processes are needed to establish the distinctive phenomenology of shadowing and antishadowing and to make the NuTeV results definitive. It is also important to map out the shadowing and antishadowing of each quark component of

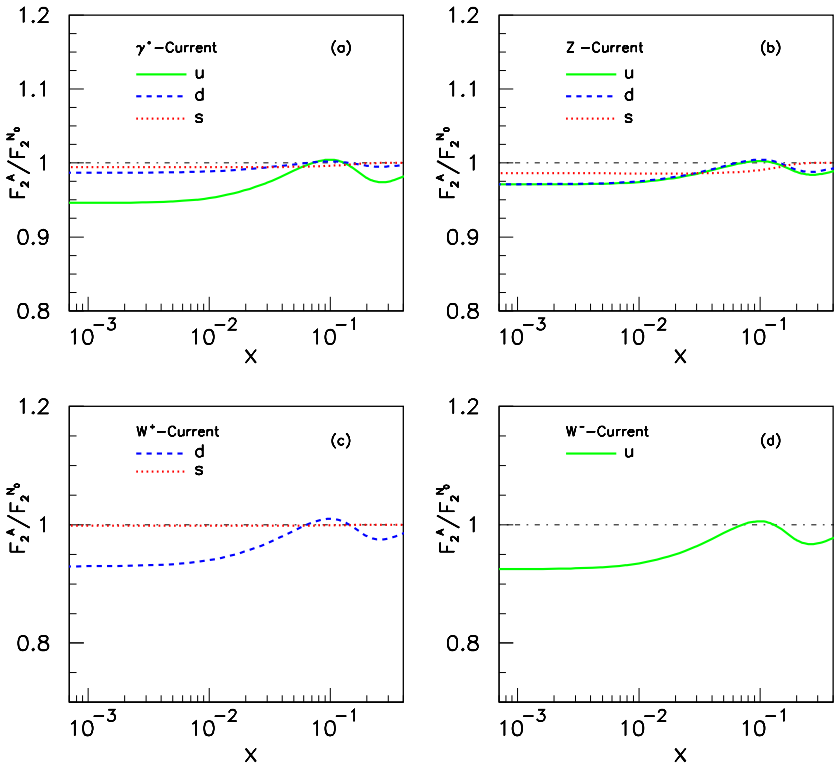

Figure 3: The quark contributions to the ratios of structure functions at $Q^2 = 1$ GeV^2. The solid, dashed and dotted curves correspond to the u, d and s quark contributions, respectively. This corresponds in our model to the nuclear dependence of the $\sigma(\overline{u}-A)$, $\sigma(\overline{d}-A)$, $\sigma(\overline{s}-A)$ cross sections, respectively. In order to stress the individual contribution of quarks, the numerator of the ratio $F_2^A/F_2^{N_0}$ shown in these two figures is obtained from the denominator by a replacement q^{N_0} into q^A for only the considered quark. As a result, the effect of antishadowing appears diminished.

the nuclear structure functions to illuminate the underlying QCD mechanisms. Such studies can be carried out in semi-inclusive deep inelastic scattering for the electromagnetic current at Hermes and at Jefferson Laboratory by tagging the flavor of the current quark or by using pion and kaon-induced Drell-Yan reactions. A new determination of $\sin^2\theta_W$ is also expected from the neutrino scattering experiment NOMAD at CERN [30]. A systematic program of measurements of the nuclear effects in charged and neutral current reactions could also be carried out in high energy electron-nucleus colliders such as HERA and eRHIC, or by using high intensity neutrino beams [31].

1.3 Structure Functions Are Not Probability Functions

As discussed above, the leading-twist contribution to DIS is affected by diffractive rescattering of a quark in the target, a coherent effect which is not included in the

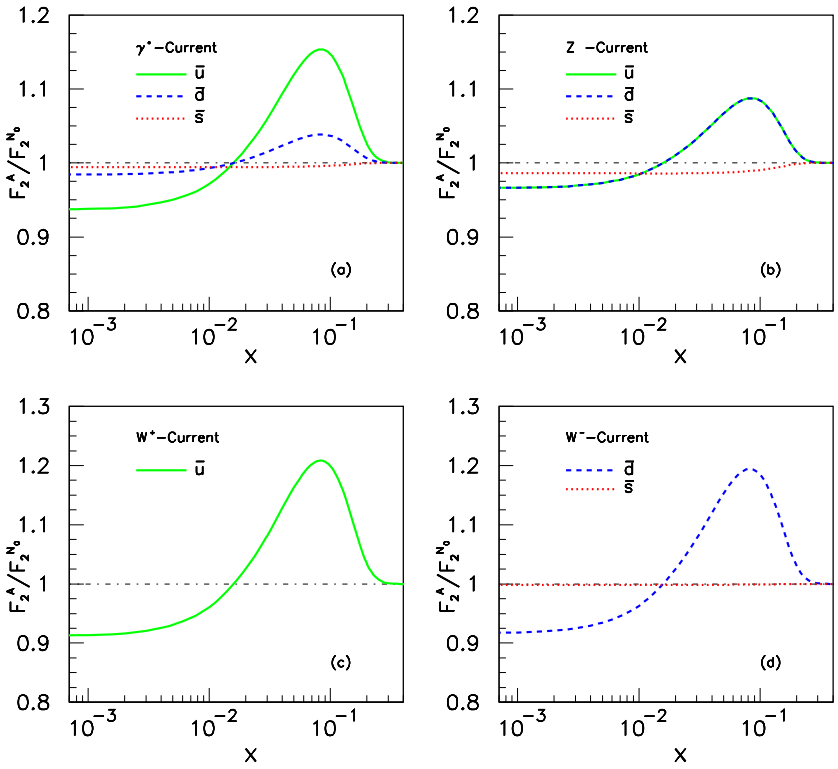

Figure 4: The anti-quark contributions to ratios of the structure functions at $Q^2 = 1$ GeV^2. The solid, dashed and dotted curves correspond to $\overline{u}$, $\overline{d}$ and $\overline{s}$ quark contributions, respectively. This corresponds in our model to the nuclear dependence of the $\sigma(u-A)$, $\sigma(d-A)$, $\sigma(s-A)$ cross sections, respectively. In order to stress the individual contribution of quarks, the numerator of the ratio $F_2^A/F_2^{N_0}$ shown in these two figures is obtained from the denominator by a replacement $\overline{q}^{N_0}$ into $\overline{q}^A$ for only the considered anti-quark.

light-front wave functions computed in isolation, even in light-cone gauge. Diffractive contributions which leave the target intact do not resolve the quark structure of the target, and thus there are contributions to structure functions which are not parton probabilities [8].

The shadowing of nuclear structure functions is due to the destructive interference between rescattering amplitudes involving on-shell intermediate states with a complex phase. In contrast, the wave function of a stable target is strictly real since it does not have on-energy-shell intermediate state configurations. The physics of shadowing is thus not included in the nuclear light-front wave functions, and a probabilistic interpretation of the DIS cross section is thus precluded.

As an alternative, one can augment the light-front wave functions with a gauge link corresponding to an external field created by the virtual photon $q\overline{q}$ pair current [32, 33]. Such a gauge link is process dependent [34], so the resulting augmented LFWFs

are not universal [8, 32, 35]. Such rescattering corrections are not contained in the target light-front wave functions computed in isolation.

2 Single-Spin Asymmetries from Final-State Interactions

Spin correlations provide a remarkably sensitive window to hadronic structure and basic mechanisms in QCD. Among the most interesting polarization effects are single-spin azimuthal asymmetries in semi-inclusive deep inelastic scattering, representing the correlation of the spin of the proton target and the virtual photon to hadron production plane: $\vec{S}_p \cdot \vec{q} \times \vec{p}_H$ [36]. Such asymmetries are time-reversal odd, but they can arise in QCD through phase differences in different spin amplitudes.

Until recently, the traditional explanation of pion electroproduction single-spin asymmetries in semi-inclusive deep inelastic scattering is that they are proportional to the transversity distribution of the quarks in the hadron h_1 [37, 38, 39] convoluted with the transverse momentum dependent fragmentation (Collins) function $H_1^\perp$, the distribution for a transversely polarized quark to fragment into an unpolarized hadron with non-zero transverse momentum [40, 41, 42, 43, 44].

Dae Sung Hwang, Ivan Schmidt and I have showed that an alternative physical mechanism for the azimuthal asymmetries also exists [10, 45, 46]. The same QCD final-state interactions (gluon exchange) between the struck quark and the proton spectators which lead to diffractive events also can produce single-spin asymmetries (the Sivers effect) in semi-inclusive deep inelastic lepton scattering which survive in the Bjorken limit. In contrast to the SSAs arising from transversity and the Collins fragmentation function, the fragmentation of the quark into hadrons is not necessary; one predicts a correlation with the production plane of the quark jet itself $\vec{S}_p \cdot \vec{q} \times \vec{p}_q$.

The final-state interaction mechanism provides an appealing physical explanation within QCD of single-spin asymmetries. Remarkably, the same matrix element which determines the spin-orbit correlation $\vec{S} \cdot \vec{L}$ also produces the anomalous magnetic moment of the proton, the Pauli form factor, and the generalized parton distribution E which is measured in deeply virtual Compton scattering. Physically, the final-state interaction phase arises as the infrared-finite difference of QCD Coulomb phases for hadron wave functions with differing orbital angular momentum. An elegant discussion of the Sivers effect including its sign has been given by Burkardt [47].

The final-state interaction effects can also be identified with the gauge link which is present in the gauge-invariant definition of parton distributions [45]. Even when the light-cone gauge is chosen, a transverse gauge link is required. Thus in any gauge the parton amplitudes need to be augmented by an additional eikonal factor incorporating the final-state interaction and its phase [46, 32]. The net effect is that it is possible to define transverse momentum dependent parton distribution functions which contain the effect of the QCD final-state interactions.

A related analysis also predicts that the initial-state interactions from gluon exchange between the incoming quark and the target spectator system lead to leading-twist single-spin asymmetries in the Drell-Yan process $H_1 H_2^{\uparrow} \to \ell^+\ell^- X$ [34, 48]. Initial-state interactions also lead to a $\cos 2\phi$ planar correlation in unpolarized Drell-Yan reactions [49].

2.1 Calculations of Single-Spin Asymmetries in QCD

Hwang, Schmidt and I have calculated [10] the single-spin Sivers asymmetry in semi-inclusive electroproduction $\gamma^* p^{\uparrow} \to HX$ induced by final-state interactions in a model of a spin-$\frac{1}{2}$ 688 proton of mass M with charged spin-$\frac{1}{2}$ and spin-0 constituents of mass m and λ, respectively, as in the QCD-motivated quark-diquark model of a nucleon. The basic electroproduction reaction is then $\gamma^* p \to q(qq)_0$. In fact, the asymmetry comes from the interference of two amplitudes which have different proton spin, but couple to the same final quark spin state, and therefore it involves the interference of tree and one-loop diagrams with a final-state interaction. In this simple model the azimuthal target single-spin asymmetry $A_{UT}^{\sin\phi}$ is given by

$$\begin{aligned} A_{UT}^{\sin\phi} &= C_F \alpha_s(\mu^2)\, \frac{\Big(\, \Delta\, M + m \,\Big)\, r_\perp}{\Big[\, \Big(\, \Delta\, M + m \,\Big)^2 \,+\, \vec{r}_\perp^{\,2} \,\Big]} \\ &\times \left[\, \vec{r}_\perp^{\,2} + \Delta(1-\Delta)(-M^2 + \frac{m^2}{\Delta} + \frac{\lambda^2}{1-\Delta}) \,\right] \\ &\times \frac{1}{\vec{r}_\perp^{\,2}}\, \ln \frac{\vec{r}_\perp^{\,2} + \Delta(1-\Delta)(-M^2 + \frac{m^2}{\Delta} + \frac{\lambda^2}{1-\Delta})}{\Delta(1-\Delta)(-M^2 + \frac{m^2}{\Delta} + \frac{\lambda^2}{1-\Delta})} \,. \end{aligned} \tag{8}$$

Here $r_\perp$ is the magnitude of the transverse momentum of the current quark jet relative to the virtual photon direction, and $\Delta = x_{Bj}$ is the usual Bjorken variable. To obtain (8) from Eq. (21) of [10], we used the correspondence $|e_1 e_2|/4\pi \to C_F \alpha_s(\mu^2)$ and the fact that the sign of the charges e_1 and e_2 of the quark and diquark are opposite since they constitute a bound state. The result can be tested in jet production using an observable such as thrust to define the momentum $q + r$ of the struck quark.

The predictions of our model for the asymmetry $A_{UT}^{\sin\phi}$ of the $\vec{S}_p \cdot \vec{q} \times \vec{p}_q$ correlation based on Eq. (8) are shown in Fig. 5. As representative parameters we take $\alpha_s = 0.3$, $M = 0.94$ GeV for the proton mass, $m = 0.3$ GeV for the fermion constituent and $\lambda = 0.8$ GeV for the spin-0 spectator. The single-spin asymmetry $A_{UT}^{\sin\phi}$ is shown as a function of Δ and $r_\perp$ (GeV). The asymmetry measured at HERMES [51] $A_{UL}^{\sin\phi} = K A_{UT}^{\sin\phi}$ contains a kinematic factor $K = \frac{Q}{\nu}\sqrt{1-y} = \sqrt{\frac{2Mx}{E}}\sqrt{\frac{1-y}{y}}$ because the proton is polarized along the incident electron direction. The resulting prediction for $A_{UL}^{\sin\phi}$ is shown in Fig. 5(b). Note that $\vec{r} = \vec{p}_q - \vec{q}$ is the momentum of the current quark

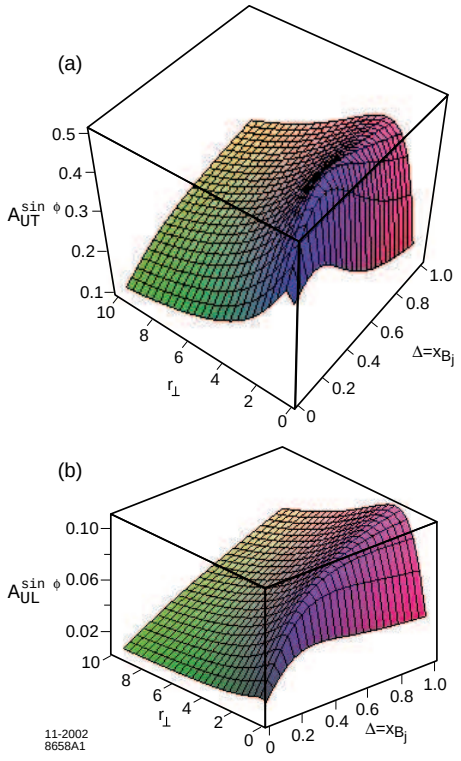

Figure 5: Model predictions for the target single-spin asymmetry $A_{UT}^{\sin\phi}$ for charged and neutral current deep inelastic scattering resulting from gluon exchange in the final state. Here $r_\perp$ is the magnitude of the transverse momentum of the outgoing quark relative to the photon or vector boson direction, and $\Delta = x_{bj}$ is the light-cone momentum fraction of the struck quark. The parameters of the model are given in the text. In (a) the target polarization is transverse to the incident lepton direction. The asymmetry in (b) $A_{UL}^{\sin\phi} = K A_{UT}^{\sin\phi}$ includes a kinematic factor $K = \frac{Q}{\nu}\sqrt{1-y}$ for the case where the target nucleon is polarized along the incident lepton direction. For illustration, we have taken $K = 0.26\sqrt{x}$, corresponding to the kinematics of the HERMES experiment [51] with $E_{lab} = 27.6$ GeV and $y = 0.5$.

jet relative to the photon momentum. The asymmetry as a function of the pion momentum $\vec{p}_\pi$ requires a convolution with the quark fragmentation function.

Since the same matrix element controls the Pauli form factor, the contribution of each quark current to the SSA is proportional to the contribution $\kappa_{q/p}$ of that quark to the proton target's anomalous magnetic moment $\kappa_p = \sum_q e_q \kappa_{q/p}$ [10, 47]. Avakian [36] has shown that the data from HERMES and Jefferson laboratory could be accounted for by the above analysis. The HERMES collaboration has recently measured the SSA in pion electroproduction using transverse target polarization [52]. The Sivers and Collins effects can be separated using planar correlations; both contributions are observed to contribute, with values not in disagreement with theory expectations.

It should be emphasized that the Sivers effect occurs even for jet production; unlike transversity, hadronization is not required. There is no Sivers effect in charged current reactions since the W only couples to left-handed quarks [53].

The corresponding single spin asymmetry for the Drell-Yan processes, such as $\pi p^\leftrightarrow$ (or $pp^\leftrightarrow$) $\to \gamma^* X \to \ell^+\ell^- X$, is due to initial-state interactions. The simplest way to get the result is applying crossing symmetry to the SIDIS processes. The result that the SSA in the Drell-Yan process is the same as that obtained in SIDIS, with the appropriate identification of variables, but with the opposite sign [45, 48].

We can also consider the SSA of e^+e^- annihilation processes such as $e^+e^- \to \gamma^* \to \pi\Lambda^\leftrightarrow X$. The Λ reveals its polarization via its decay $\Lambda \to p\pi^-$. The spin of the Λ is normal to the decay plane. Thus we can look for a SSA through the T-odd correlation $\epsilon_{\mu\nu\rho\sigma} S_\Lambda^\mu p_\Lambda^\nu q_{\gamma^*}^\rho p_\pi^\sigma$. This is related by crossing to SIDIS on a Λ target.

Measurements from Jefferson Lab [54] also show significant beam single spin asymmetries in deep inelastic scattering. Afanasev and Carlson [55] have recently shown that this asymmetry is due to the interference of longitudinal and transverse photoabsorption amplitudes which have different phases induced by the final-state interaction between the struck quark and the target spectators just as in the calculations of Ref. [10]. Their results are consistent with the experimentally observed magnitude of this effect. Thus similar FSI mechanisms involving quark orbital angular momentum appear to be responsible for both target and beam single-spin asymmetries.

3 Heavy Quark Components of the Proton Structure Function

In the simplest treatment of deep inelastic scattering, nonvalence quarks are produced via gluon splitting and DGLAP evolution. However, in the full theory, heavy quarks are multiply connected to the valence quarks [56]. In fact, the multiple interactions of the sea quarks produce an asymmetry of the strange and anti-strange distributions in the nucleon due to their different interactions with the other quark constituents. A QED analogy is the distribution of τ^+ and τ^- in a higher Fock state of muonium μ^+e^-. The τ^- is attracted to the μ^+ thus asymmetrically distorting its momentum

distribution.

The probability for Fock states of a light hadron such as the proton to have an extra heavy quark pair decreases as $1/m_Q^2$ in non-Abelian gauge theory [57, 58]. The relevant matrix element is the cube of the QCD field strength $G^3_{\mu nu}$. This is in striking contrast to abelian gauge theory where the relevant operator is $F^4_{\mu\nu}$ and the probability of intrinsic heavy leptons in QED bound state is suppressed as $1/m_\ell^4$. The intrinsic Fock state probability is maximized at minimal off shellness. The maximum probability occurs at $x_i = m_\perp^i / \sum_{j=1}^n m_\perp^j$; i.e., when the constituents have equal rapidity. Thus the heaviest constituents have the highest light-cone momentum fractions x. Intrinsic charm thus predicts that the charm structure function has support at large x_{bj} in excess of DGLAP extrapolations [56]; this is in agreement with the EMC measurements [59]. As discussed in the next section, the diffractive dissociation of the intrinsic charm Fock state leads to leading charm hadron production and fast charmonium production in agreement with measurements [60]. The production cross section for the double charmed Ξ_{cc}^+ baryon [61] and the production of double $J/\psi's$ appears to be consistent with the dissociation and coalescence of double IC Fock states [62, 63]. Intrinsic charm can also explain the $J/\psi \to \rho\pi$ puzzle [64], and it affects the extraction of suppressed CKM matrix elements in B decays [65]. Intrinsic charm can also enhance the production probability of Higgs bosons at hadron colliders from processes such as $gc \to Hc$. It is thus critical for new experiments (HERMES, HERA, COMPASS) to definitively establish the phenomenology of the charm structure function at large x_{bj}.

4 Diffraction Dissociation as a Tool to Resolve Hadron Substructure

Diffractive multi-jet production in heavy nuclei provides a novel way to measure the shape of light-front Fock state wave functions and test color transparency [66]. For example, consider the reaction [67, 68] $\pi A \to \mathrm{Jet}_1 + \mathrm{Jet}_2 + A'$ at high energy where the nucleus A' is left intact in its ground state. The transverse momenta of the jets balance so that $\vec{k}_{\perp i} + \vec{k}_{\perp 2} = \vec{q}_\perp < R^{-1}{}_A$. The light-cone longitudinal momentum fractions also need to add to $x_1 + x_2 \sim 1$. Diffractive dissociation on a nucleus also requires that the energy of the beam has to be sufficiently large such that the momentum transfer to the nucleus $\Delta p_L = \frac{\Delta M^2}{2E_{lab}}$ is smaller than the inverse nuclear size R_A. The process can then occur coherently in the nucleus.

Because of color transparency, the valence wave function of the pion with small impact separation will penetrate the nucleus with minimal interactions, diffracting into jet pairs [67]. The $x_1 = x$, $x_2 = 1 - x$ dependence of the di-jet distributions will thus reflect the shape of the pion valence light-cone wave function in x; similarly, the $\vec{k}_{\perp 1} - \vec{k}_{\perp 2}$ relative transverse momenta of the jets gives key information on the second transverse momentum derivative of the underlying shape of the valence

pion wavefunction [68, 69]. The diffractive nuclear amplitude extrapolated to $t = 0$ should be linear in nuclear number A if color transparency is correct. The integrated diffractive rate will then scale as $A^2/R_A^2 \sim A^{4/3}$. This is in fact what has been observed by the E791 collaboration at FermiLab for 500 GeV incident pions on nuclear targets [70]. The measured momentum fraction distribution of the jets is found to be approximately consistent with the shape of the pion asymptotic distribution amplitude, $\phi_\pi^{\rm asympt}(x) = \sqrt{3} f_\pi x(1-x)$ [71]. Data from CLEO [72] for the $\gamma\gamma^* \to \pi^0$ transition form factor also favor a form for the pion distribution amplitude close to the asymptotic solution to its perturbative QCD evolution equation [73, 74, 75].

The concept of high energy diffractive dissociation can be generalized to provide a tool to materialize the individual Fock states of a hadron or photon. For example, the diffractive dissociation of a high energy proton on a nucleus $pA \to XA'$ where the diffractive system is three jets $X = qqq$ can be used to determine the valence light-front wavefunction of the proton.

4.1 Diffractive Dissociation and Hidden Color in Nuclear Wavefunctions

In the case of a deuteron projectile, one can study diffractive processes such as $dA \to pnA'$ or $dA \to \pi^- pp$ to measure the mesonic Fock state of a nuclear wavefunction. At small hadron transverse momentum, diffractive dissociation of the deuteron should be controlled by conventional nuclear interactions; however at large relative k_T, the diffractive system should be sensitive to "hidden color" components of the deuteron wavefunction.

In general, the six-quark wavefunction of a deuteron is a mixture of five different color-singlet states. The dominant color configuration at large distances corresponds to the usual proton-neutron bound state where transverse momenta are of order $\vec{k}^2 \sim 2M_d\epsilon_{BE}$. However, at small impact space separation, all five Fock color-singlet components eventually acquire equal weight, i.e., the deuteron wavefunction evolves to 80% hidden color. At high Q^2 the deuteron form factor is sensitive to wavefunction configurations where all six quarks overlap within an impact separation $b_{\perp i} < \mathcal{O}(1/Q)$. The derivation of the evolution equation for the deuteron distribution amplitude and its leading anomalous dimension γ is given in Ref. [76]. The relatively large normalization of the deuteron form factor observed at large Q^2 [77], as well as the presence of two mass scales in the scaling behavior of the reduced deuteron form factor [78] $f_d(Q^2) = F_d(Q^2)/F^2(Q^2/4)$ suggests sizable hidden-color contributions in the deuteron wavefunction.

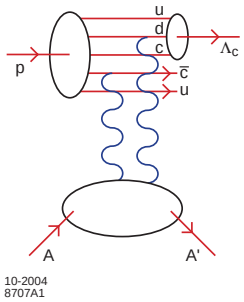

Figure 6: Production of forward heavy baryons by diffractive dissociation.

4.2 Diffractive Dissociation and Heavy Quark Production

Diffractive dissociation is particularly relevant to the production of leading heavy quark states. The projectile proton can be decomposed as a sum over all of its Fock state components. The diffractive dissociation of the intrinsic charm $|uudc\overline{c}>$ Fock state of the proton on a nucleus can produce a leading heavy quarkonium state at high $x_F = x_c + x_{\overline{c}}$ in $pA \to J/\psi X A'$ since the c and $\overline{c}$ can readily coalesce into the charmonium state. Since the constituents of a given intrinsic heavy-quark Fock state tend to have the same rapidity, coalescence of multiple partons from the projectile Fock state into charmed hadrons and mesons is also favored. For example, as illustrated in fig. 6, one can produce leading Λ_c at high x_F and low p_T from the coalescence of the udc constituents of the projectile IC Fock state. A similar coalescence mechanism was used in atomic physics to produce relativistic antihydrogen in $\overline{p}A$ collisions [79]. This phenomena is important not only for understanding heavy-hadron phenomenology, but also for understanding the sources of neutrinos in astrophysics experiments [80].

The charmonium state will be produced at small transverse momentum and high x_F with a characteristic $A^{2/3}$ nuclear dependence. This forward contribution is in addition to the A^1 contribution derived from the usual PQCD fusion at small x_F. Because of these two components, the cross section violates perturbative QCD factorization for hard inclusive reactions [81]. This is consistent with the observed two-component cross section for charmonium production observed by the NA3 collaboration at CERN [82].

The production cross section for the double-charm Ξ_{cc}^+ baryon [61] and the production of J/ψ pairs appears to be consistent with the diffractive dissociation and coalescence of double IC Fock states [63, 62]. It is unlikely that the appearance of two heavy quarks at high x_F could be explained by the "color drag model" used in PYTHIA simulations [83] in which the heavy quarks are accelerated from low to high x by the fast valence quarks. It is also conceivable that the observations [84] of Λ_b at high x_F at the ISR in high energy pp collisions could be due to the diffractive dissociation and coalescence of the "intrinsic bottom" $|uudb\overline{b}>$ Fock states of the proton.

Acknowledgements

It is a pleasure to thank Professors Bill Gary and Ken Barish and the other organizers of ISMD 2004 for their hospitality in Sonoma. I also thank my collaborators, particularly Rikard Enberg, Fred Goldhaber, Paul Hoyer, Dae Sung Hwang, Gunnar Ingelman, Marek Karliner, and Ivan Schmidt. This work was supported by the Department of Energy, contract No. DE-AC02-76SF00515.

References

[1] For a review see S. J. Brodsky, H. C. Pauli and S. S. Pinsky, Phys. Rept. **301**, 299 (1998) [arXiv:hep-ph/9705477].

[2] J. Carbonell, B. Desplanques, V. A. Karmanov, and J. F. Mathiot, Phys. Rep. **300**, 215 (1998) [arXiv:nucl-th/9804029].

[3] H. Abramowicz, in *Proc. of the 19th Intl. Symp. on Photon and Lepton Interactions at High Energy LP99* ed. J.A. Jaros and M.E. Peskin, Int. J. Mod. Phys. A **15S1**, 495 (2000) [eConf **C990809**, 495 (2000)] [arXiv:hep-ph/0001054].

[4] C. Adloff *et al.* [H1 Collaboration], Z. Phys. C **76**, 613 (1997) [arXiv:hep-ex/9708016].

[5] J. Breitweg *et al.* [ZEUS Collaboration], Eur. Phys. J. C **6**, 43 (1999) [arXiv:hep-ex/9807010].

[6] For a review, see J. Raufeisen, arXiv:hep-ph/0009358.

[7] S. J. Brodsky, L. Frankfurt, J. F. Gunion, A. H. Mueller and M. Strikman, Phys. Rev. D **50**, 3134 (1994) [arXiv:hep-ph/9402283].

[8] S. J. Brodsky, P. Hoyer, N. Marchal, S. Peigne and F. Sannino, Phys. Rev. D **65**, 114025 (2002) [arXiv:hep-ph/0104291].

[9] S. J. Brodsky, R. Enberg, P. Hoyer and G. Ingelman, arXiv:hep-ph/0409119.

[10] S. J. Brodsky, D. S. Hwang and I. Schmidt, Phys. Lett. B **530**, 99 (2002) [arXiv:hep-ph/0201296].

[11] R. J. Glauber, Phys. Rev. **100**, 242 (1955).

[12] V. N. Gribov, Sov. Phys. JETP **30**, 709 (1970) [Zh. Eksp. Teor. Fiz. **57**, 1306 (1969)].

[13] V. N. Gribov, Sov. Phys. JETP **29**, 483 (1969) [Zh. Eksp. Teor. Fiz. **56**, 892 (1969)].

[14] L. Stodolsky, Phys. Rev. Lett. **18**, 135 (1967).

[15] S. J. Brodsky and J. Pumplin, Phys. Rev. **182** (1969) 1794.

[16] S. J. Brodsky and H. J. Lu, Phys. Rev. Lett. **64** (1990) 1342.

[17] B. L. Ioffe, Phys. Lett. B **30**, 123 (1969).

[18] L. L. Frankfurt and M. I. Strikman, Nucl. Phys. B **316**, 340 (1989).

[19] B. Z. Kopeliovich, J. Raufeisen and A. V. Tarasov, Phys. Lett. B **440**, 151 (1998) [arXiv: hep-ph/9807211].

[20] D. E. Kharzeev and J. Raufeisen, nucl-th/0206073, and references therein.

[21] A. H. Mueller and A. I. Shoshi, arXiv:hep-ph/0402193.

[22] J. w. Qiu and I. Vitev, arXiv:hep-ph/0405068.

[23] A. D. Martin, M. G. Ryskin and G. Watt, arXiv:hep-ph/0406224.

[24] M. Ruspa, Acta Phys. Polon. B **35**, 473 (2004).

[25] S. J. Brodsky and H. J. Lu, Phys. Rev. Lett. **64**, 1342 (1990).

[26] J. Kuti and V. F. Weisskopf, Phys. Rev. D **4**, 3418 (1971).

[27] M. Arneodo, Phys. Rept. **240**, 301 (1994).

[28] S. J. Brodsky, I. Schmidt and J. J. Yang, arXiv:hep-ph/0409279.

[29] K. S. McFarland *et al.*, Int. J. Mod. Phys. A **18**, 3841 (2003).

[30] R. Petti, (NOMAD collaboration) presented at ICHEP(2004).

[31] Steve Geer, hep-ph/0210113, Talk given at 4th NuFact '02 Workshop (Neutrino Factories based on Muon Storage Rings), London, England, 1-6 Jul 2002.

[32] A. V. Belitsky, X. Ji and F. Yuan, Nucl. Phys. B **656**, 165 (2003) [arXiv:hep-ph/0208038].

[33] J. C. Collins and A. Metz, arXiv:hep-ph/0408249.

[34] J. C. Collins, Phys. Lett. B **536**, 43 (2002) [arXiv:hep-ph/0204004].

[35] J. C. Collins, arXiv:hep-ph/0304122.

[36] H. Avakian [CLAS Collaboration], *Workshop on Testing QCD through Spin Observables in Nuclear Targets, Charlottesville, Virginia, 18-20 Apr 2002*

[37] R.L. Jaffe, hep-ph/9602236.

[38] D. Boer, Nucl. Phys. Proc. Suppl. **105**, 76 (2002) [hep-ph/0109221].

[39] D. Boer, Nucl. Phys. **A 711**, 21 (2002) [hep-ph/0206235].

[40] J.C. Collins, Nucl. Phys. **B 396**, 161 (1993).

[41] V. Barone, A. Drago and P.G. Ratcliffe, Phys. Rept. **359**, 1 (2002).

[42] B. Q. Ma, I. Schmidt and J. J. Yang, Phys. Rev. D **66**, 094001 (2002) [arXiv:hep-ph/0209114].

[43] G. R. Goldstein and L. Gamberg, arXiv:hep-ph/0209085.

[44] L. P. Gamberg, G. R. Goldstein and K. A. Oganessyan, Phys. Rev. D **67**, 071504 (2003) [arXiv:hep-ph/0301018].

[45] J.C. Collins, Phys. Lett. **B 536**, 43 (2002).

[46] X. Ji and F. Yuan, Phys. Lett. **B 543**, 66 (2002).

[47] M. Burkardt, arXiv:hep-ph/0408009.

[48] S.J. Brodsky, D.S. Hwang and I. Schmidt, Nucl. Phys. **B 642**, 344 (2002).

[49] D. Boer, S. J. Brodsky and D. S. Hwang, Phys. Rev. D **67**, 054003 (2003) [arXiv:hep-ph/0211110].

[50] D.W. Sivers, Phys. Rev. **D 43**, 261 (1991).

[51] A. Airapetian *et al.* [HERMES Collaboration], Phys. Rev. Lett. **84**, 4047 (2000).

[52] A. Airapetian *et al.* [HERMES Collaboration], arXiv:hep-ex/0408013.

[53] S. J. Brodsky, D. S. Hwang and I. Schmidt, Phys. Lett. B **553**, 223 (2003) [arXiv:hep-ph/0211212].

[54] H. Avakian *et al.* [CLAS Collaboration], arXiv:hep-ex/0301005.

[55] A. Afanasev and C. E. Carlson, arXiv:hep-ph/0308163.

[56] S. J. Brodsky, P. Hoyer, C. Peterson and N. Sakai, Phys. Lett. B **93**, 451 (1980).

[57] M. Franz, V. Polyakov and K. Goeke, Phys. Rev. D **62**, 074024 (2000) [arXiv:hep-ph/0002240].

[58] S. J. Brodsky, J. C. Collins, S. D. Ellis, J. F. Gunion and A. H. Mueller, DOE/ER/40048-21 P4 *Proc. of 1984 Summer Study on the SSC, Snowmass, CO, Jun 23 - Jul 13, 1984*

[59] B. W. Harris, J. Smith and R. Vogt, Nucl. Phys. B **461**, 181 (1996) [arXiv:hep-ph/9508403].

[60] J. C. Anjos, J. Magnin and G. Herrera, Phys. Lett. B **523**, 29 (2001) [arXiv:hep-ph/0109185].

[61] A. Ocherashvili *et al.* [SELEX Collaboration], arXiv:hep-ex/0406033.

[62] R. Vogt and S. J. Brodsky, Phys. Lett. B **349**, 569 (1995) [arXiv:hep-ph/9503206].

[63] S. J. Brodsky, A. S. Goldhaber, and M. Karliner, in progress.

[64] S. J. Brodsky and M. Karliner, Phys. Rev. Lett. **78**, 4682 (1997) [arXiv:hep-ph/9704379].

[65] S. J. Brodsky and S. Gardner, Phys. Rev. D **65**, 054016 (2002) [arXiv:hep-ph/0108121].

[66] S. J. Brodsky and A. H. Mueller, Phys. Lett. B **206**, 685 (1988).

[67] G. Bertsch, S. J. Brodsky, A. S. Goldhaber and J. F. Gunion, Phys. Rev. Lett. **47**, 297 (1981).

[68] L. Frankfurt, G. A. Miller and M. Strikman, Found. Phys. **30**, 533 (2000) [arXiv:hep-ph/9907214].

[69] N. N. Nikolaev, W. Schafer and G. Schwiete, Phys. Rev. D **63**, 014020 (2001) [arXiv:hep-ph/0009038].

[70] E. M. Aitala *et al.* [E791 Collaboration], Phys. Rev. Lett. **86**, 4773 (2001) [arXiv:hep-ex/0010044].

[71] E. M. Aitala *et al.* [E791 Collaboration], Phys. Rev. Lett. **86**, 4768 (2001) [arXiv:hep-ex/0010043].

[72] J. Gronberg *et al.* [CLEO Collaboration], Phys. Rev. D **57**, 33 (1998) [arXiv:hep-ex/9707031].

[73] G. P. Lepage and S. J. Brodsky, Phys. Lett. B **87**, 359 (1979).

[74] A. V. Efremov and A. V. Radyushkin, Theor. Math. Phys. **42**, 97 (1980) [Teor. Mat. Fiz. **42**, 147 (1980)].

[75] G. P. Lepage and S. J. Brodsky, Phys. Rev. D **22**, 2157 (1980).

[76] S. J. Brodsky, C. R. Ji and G. P. Lepage, Phys. Rev. Lett. **51**, 83 (1983).

[77] G. R. Farrar, K. Huleihel and H. y. Zhang, Phys. Rev. Lett. **74**, 650 (1995).

[78] S. J. Brodsky and B. T. Chertok, Phys. Rev. D **14**, 3003 (1976).

[79] C. T. Munger, S. J. Brodsky and I. Schmidt, Phys. Rev. D **49**, 3228 (1994).

[80] F. Halzen, arXiv:astro-ph/0402083.

[81] P. Hoyer, M. Vanttinen and U. Sukhatme, Phys. Lett. B **246**, 217 (1990).

[82] J. Badier *et al.* [NA3 Collaboration], Phys. Lett. B **104**, 335 (1981).

[83] B. Andersson, G. Gustafson, G. Ingelman and T. Sjostrand, Phys. Rept. **97**, 31 (1983).

[84] G. Bari *et al.*, Nuovo Cim. A **104**, 1787 (1991).